Electrochemical Properties of Catechin in Non-Aqueous Media

Anna Masek[1], Ewa Chrzescijanska[2], Marian Zaborski[1]*

[1] Technical University of Lodz, Institute of Polymer and Dye Technology, Faculty of Chemistry, 90-924 Lodz, ul Stefanowskiego 12/16, Poland
[2] Technical University of Lodz, Institute of General and Ecological Chemistry, Faculty of Chemistry, 90-924 Lodz, ul Zeromskiego 116, Poland
[*]E-mail: anna.masek@p.lodz.pl

The oxidation of flavonoids is of great interest because flavonoids act as antioxidants scavenging free radicals through the electron transfer processes. Electrochemical oxidation of catechin at a platinum (Pt) electrode was investigated using cyclic (CV) and differential pulse (DPV) voltammetry methods. The oxidation of catechin is an irreversible two-step process. The effect of scan rate and substrate concentration on the electrode reactions was determined. The oxidation process and its kinetics have been investigated. Certain parameters of the substrate electrooxidation, i.e., the heterogeneous rate constant and the charge transfer coefficient, were calculated. Based on the experimental results and quantum chemistry calculations, the electrooxidative mechanisms of catechin were proposed. The results underline the importance of electrochemical methods in the clarification of the oxidation processes of bioactive molecules. The properties of catechin in a homogeneous environment were investigated using FTIR spectroscopy and DSC analysis.

Keywords: catechin; electrooxidation; Pt electrode; FTIR spectroscopy

1. INTRODUCTION

Flavonoids are natural antioxidants that belong to a considerably greater group of polyphenols. The main sources of flavonoids are fruits and vegetables as well as tea. Catechin is a flavonoid present in green tea and wine [1, 2]. It is characterised by good antioxidising properties [3, 4]. Catechins allow continual neutralisation of the adverse effects of free radicals by decreasing the number of free radicals [5, 6]. Another important dietary merit of catechins is that they are easily absorbed by the human digestive tract, which results faster and better regeneration of body cells, thereby slowing down the ageing process and energising cells. Catechins also help strengthen the human immune system [7, 8]. Drinking green tea daily allows one to eliminate hazardous toxins and reinforces the immune system.

Catechnis are of importance in the protection of human skin against solar radiation. They absorb excess UV radiation and decrease the risk of skin cancer, regulating the moisture of the skin and preventing pathological dermal changes [9]. Scientists also believe that catechins show a positive effect on decreasing low-density lipoproteins (LDL cholesterol) [10, 11]. Recent studies also indicate that catechins play a significant role in maintaining good vision. Moreover, catechins show antibacterial and antiviral effects [12-14]. Historically, catechins have been used in both medicine and body care to slow the ageing process and maintain health. Figure 1 shows the structure of catechin. It consists of benzene rings A and B; there is much evidence that the catechol group in ring B is the antioxidant active moiety. Catechin has two different pharmacophores: the catechol moiety in ring B and resorcinol group in the ring A. Also, an OH group is present at position 3 in ring C [6, 15].

Several techniques, such as high-performance liquid chromatography (HPLC) along with electrochemical detection [16-18], chemiluminescence detection [19], and fluorescence detection [17] have been previously used to characterise and quantify catechin. However, electroanalytical methods of detection and characterisation of organic compounds have recently attracted great attention [20-23]. The electrochemical analyses have many advantages over conventional methods. They are relatively simple, very accurate, and sensitive, and they are low-cost and require only a short analysis time [24-29]. In recent years, the identification and characterisation of catechin by electrochemical methods have both drawn attention due to the precision and simplicity of the methods [30-32]. Electrochemical measurements are fundamental for determining the physicochemical parameters of studied compounds (e.g., the redox potential, the number of electrons transferred, rate constants of electrode reactions, etc.) [33-36] and are useful for determining the electrooxidation and electroreduction mechanisms. [37-42].

The aim of this study was to determine the electrochemical behaviour of catechin during electrooxidation at a platinum electrode in non-aqueous media. The effects of the scan rate and the substrate concentration on the catechin electrode reactions were investigated using cyclic (CV) and differential pulse voltammetry (DPV). Structural investigations of catechin were conducted using FTIR spectroscopy and DSC analysis.

2. EXPERIMENTAL

2.1. Chemicals

Pure catechin ($C_{15}H_{14}O_6$, 2*R*,3*S*)-2-(3,4-dihydroxyphenyl)-3,4-dihydro-2*H*-chromene-3,5,7-triol) was obtained commercially (Sigma-Aldrich, Germany) and used as received. The chemical used for the preparation of the catechin solutions was acetonitrile (CH_3CN) pure p.a. (POCh Gliwice, Poland). Tetrabutylammonium perchlorate ((C_4H_9)$_4$NClO$_4$) (Fluka, Germany) was used as a supporting electrolyte. The concentrations of the catechin solutions ranged from 1×10^{-3} to 5×10^{-3} mol L^{-1}. All reagents used were of analytical grade.

2.2. Measurement methods

        Cyclic voltammetry (CV) and differential pulse voltammetry (DPV) were performed with an Autolab controlled by GPES software, version 4.8 (EcoChemie, The Netherlands). A three-electrode system was used for the measurements. Platinum was used as the working and auxiliary electrodes. The electrode potential was measured against a ferricinium/ferrocene reference electrode (Fc^+/Fc). Before measurements were taken, the solutions were purged with argon to remove any dissolved oxygen. During measurements, an argon blanket was kept over the solutions. The effect of the scan rate and the substrate concentration on the electrooxidation of catechin in a non-aqueous medium was assessed. All of the experiments were performed at room temperature.

        FTIR analysis: IR spectra were recorded within the wavelength range of $3000 – 700$ cm^{-1} using an FTIR Nicolet 6700 FTIR (Thermo Scientific). The measurement parameters were as follows: 128 scans; resolution was set to 8 cm^{-1}; DTGS/KBr detector was employed. The FT–Raman spectrum of the compound was also recorded in the range of $3000 – 1000$ cm^{-1}.

        The thermo-gravimetric analysis of catechin was performed using a Mettler Toledo TGA/DSC1 apparatus, and the measurements were performed under argon from $25 – 500°C$ at a nitrogen flow rate of $1.2 – 1.4$ l/h and a heating rate of $10°C/min$.

3. RESULTS AND DISCUSSION

3.1. Voltammetric behaviour of catechin

        Voltammetric methods are frequently used for the characterisation of electroactive systems. The oxidation reactions of catechin at the platinum electrode were studied by CV and DPV (characterised by higher resolution) voltammetry, illustrated in Fig. 1. Within the potential range where the compound oxidation peaks appear, the supporting electrolyte (0.1 mol L^{-1} $(C_4H_9)_4NClO_4$ in acetonitrile) shows no peaks (Fig. 1, curve 3).
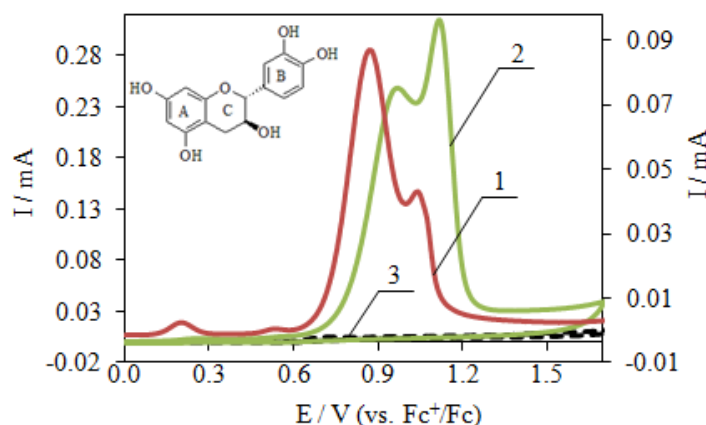

Figure 1. Voltammograms of catechin electrooxidation at a Pt electrode: curve 1 – differential pulse voltammogram; curve 2 – cyclic voltammogram; curve 3 – cyclic voltammogram recorded in the supporting electrolyte; $c = 2 \times 10^{-3}$ mol L^{-1} in 0.1 mol L^{-1} $(C_4H_9)_4NClO_4$ in acetonitrile, $v = 0.02$ V s^{-1}.

The voltammograms presented in Fig. 1 (curves 1 and 2) show that catechin is likely irreversibly oxidised in at least two steps at potentials lower than the electrolyte decomposition potentials. To check whether the substrate is adsorbed onto the electrode, DPV were recorded. DPV diminishes surface effects such as adsorption on the electrode [36] and provides higher resolution data. Two peaks in the DPV voltammogram (Fig. 1, curve 1) indicate the diffusion of catechin electrooxidation. The half-wave potential ($E_{1/2}$) of the first step of catechin oxidation, as determined by CV, is 0.89 V. This corresponds to the peak potential from the DPV measurements. The half-wave potential ($E_{1/2}$) of the second step is 1.09 V. The value of $E_{1/2}$ shifts toward more positive values with increasing scan rate showing the increasing irreversibility of the process.

3.2. An effect of scan rate

Scan rate is a parameter that significantly affects the electrooxidation of various compounds [24, 25, 43]. Thus, investigations of catechin electrooxidation included determination of the scan rate effect. The scan rate effect was investigated from 0.01 to 0.5 V s^{-1}. To characterise the electrode reaction of the catechin electrooxidation, two relationships were determined: (1) i_p vs. the square root of the scan rate ($v^{1/2}$) and (2) logarithm of i_p vs. logarithm of the scan rate (ln v). These relationships aid in determining whether the electrode reaction is controlled by adsorption or diffusion of the substrate to the electrode surface. Fig. 2 shows this relationship for the first step of catechin electrooxidation in $(C_4H_9)_4NClO_4$ in acetonitrile. If an electrode reaction is controlled by diffusion, then i_p vs. $v^{1/2}$ is linear and intercepts the origin. If this dependence does not cross the origin, the electrode reaction is controlled by adsorption [44-46].
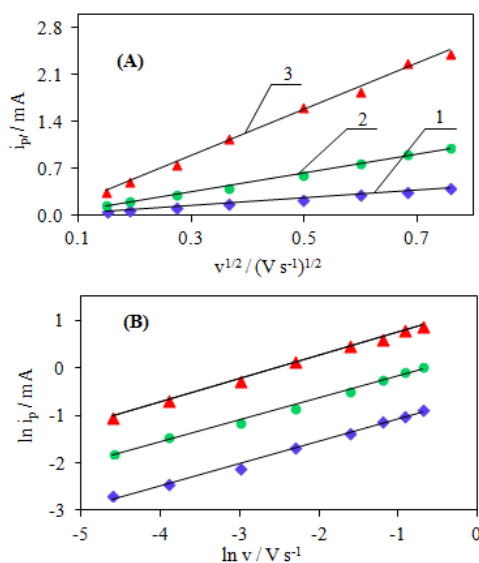

Figure 2. (**A**) Dependence of the peak anodic current (i_p) on the square root of the potential scan rate (v). (**B**) Dependence of peak anodic current on the potential scan rate in double logarithm coordinates for the oxidation of catechin at a Pt electrode in 0.1 mol L^{-1} $(C_4H_9)_4NClO_4$ in acetonitrile; curve 1: c = 1 × 10^{-3} mol L^{-1}; curve 2: c = 2 × 10^{-3} mol L^{-1}; curve 3: c = 5 × 10^{-3} mol L^{-1}.

When the scan rate ranges from 0.01 to 0.5 V s^{-1}, the anodic peak currents of catechin electrooxidation depend linearly on the square root of the scan rate (Fig. 2A) and are described by the following equations:

$i_p = \{0.570\,[v\,(V\,s^{-1})]^{1/2}\}$ mA + 0.004 mA, $R^2 = 0.998$ for $c = 1 \times 10^{-3}$ mol L^{-1};

$i_p = \{1.406\,[v\,(V\,s^{-1})]^{1/2}\}$ mA + 0.009 mA, $R^2 = 0.996$ for $c = 2 \times 10^{-3}$ mol L^{-1};

$i_p = \{3.443\,[v\,(V\,s^{-1})]^{1/2}\}$ mA + 0.031 mA, $R^2 = 0.996$ for $c = 5 \times 10^{-3}$ mol L^{-1}.

The lines described by the equations do not intercept the origin and could indicate that the electrode reaction is adsorption-controlled. However, the linear relationships of ln i_p vs. ln v presented in Fig. 2B and described by the equations:

$\ln i_p = \{0.471 \ln v\,(V\,s^{-1})\}$ mA - 0.596 mA, $R^2 = 0.994$ for $c = 1 \times 10^{-3}$ mol L^{-1};

$\ln i_p = \{0.464 \ln v\,(V\,s^{-1})\}$ mA + 0.294 mA, $R^2 = 0.994$ for $c = 2 \times 10^{-3}$ mol L^{-1};

$\ln i_p = \{0.493 \ln v\,(V\,s^{-1})\}$ mA + 1.249 mA, $R^2 = 0.998$ for $c = 5 \times 10^{-3}$ mol L^{-1},

do not confirm this conclusion.

The slope of this linear relationship is 0.475 ± 0.2 and indicates that the reaction of catechin electrooxidation is diffusion-controlled.

An effect of the scan rate on the potential of catechin electrooxidation was also investigated. Fig. 3A presents the peak potential (E$_p$) vs. the scan rate (v) for catechin electrooxidation. These relationships show that the anodic peak potentials shift toward more positive values if the scan rate increases and indicates the process is irreversible.
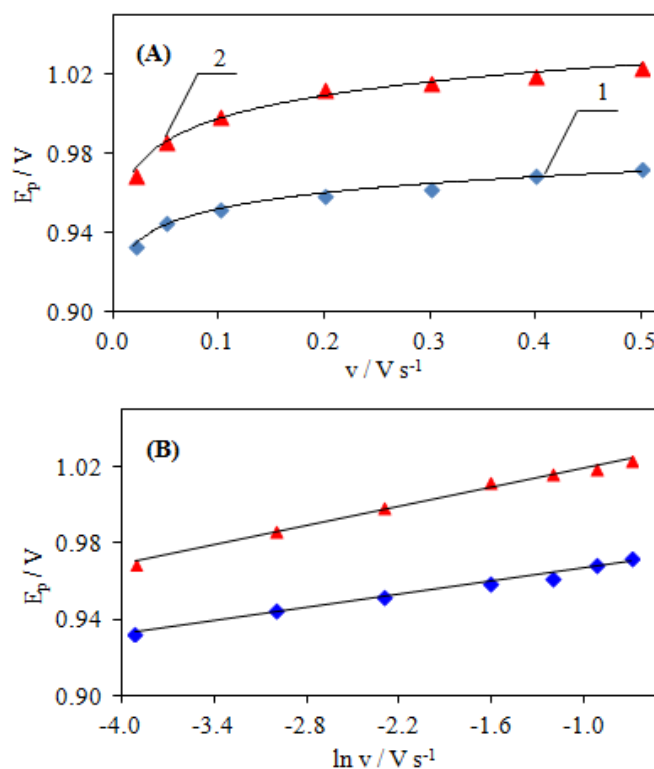

Figure 3. (A) Dependence of anodic (E$_p$) peak potential on the scan rate (*v*) for the oxidation of catechin in 0.1 mol L^{-1} (C$_4$H$_9$)$_4$NClO$_4$ in acetonitrile at a Pt electrode. (B) Dependence of E$_p$ on ln *v*; curve 1: $c = 1 \times 10^{-3}$ mol L^{-1}, curve 2: $c = 2 \times 10^{-3}$ mol L^{-1}.

Moreover, the value of the electron transfer coefficient (βn_β) for the reaction of catechin electrooxidation was calculated according to the following equation [35, 40-41]:

$$E_p = (\frac{RT}{2\beta n_\beta F})\ln v + const$$

where E_p is the peak potential (V), R is the universal gas constant (8.314J K^{-1} mol^{-1}), F is the Faraday constant (96,487 C mol^{-1}), T is temperature (298 K), βn_β is the anodic transfer coefficient, and v is the scan rate (V s^{-1}).

This equation can be applied to a completely irreversible diffusion-controlled process. The relationships of E_p vs. ln v presented in Fig. 3B are linear and are expressed by the following equations:

$E_p = \{0.012 \text{ [ln v (V s}^{-1})]\}V + 0.877 \text{ (V)}$ $R^2 = 0.989$ for c = 1 × 10^{-3} mol L^{-1};
$E_p = \{0.016 \text{ [ln v (V s}^{-1})]\}V + 0.829 \text{ (V)}$ $R^2 = 0.992$ for c = 2 × 10^{-3} mol L^{-1}.

The dependence of the peak anodic potential on the logarithm of the potential scan rate (Fig. 3B) is used to calculate the value of the anodic transfer coefficient (βn_β). Assuming that the number of electrons, n, transferred in the rate-limiting step is 1, the transfer coefficient, β, is estimated as 0.80±0.05. If we assumed n = 2, β would then be equal to 0.40±0.05.

3.3. Kinetic parameters for the electrooxidation of catechin

The effect of the catechin concentration on its electrooxidation was investigated using concentrations ranging from 1 × 10^{-3} to 5 × 10^{-3} mol L^{-1}.
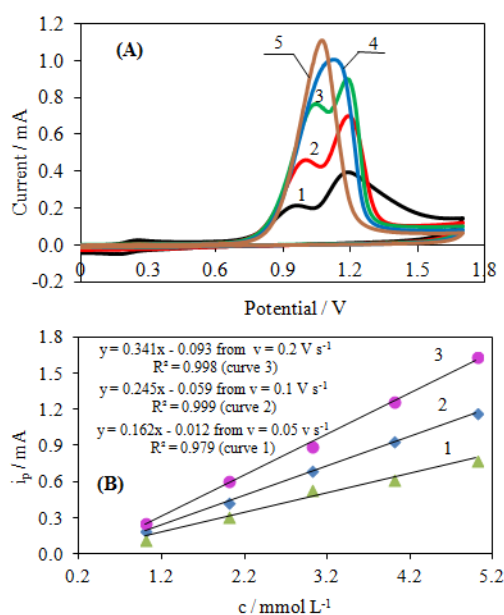

Figure 4. (A) Cyclic voltammograms of catechin oxidation at a Pt electrode; v = 0.1 V s^{-1} in 0.1 mol L^{-1} (C$_4$H$_9$)$_4$NClO$_4$ in acetonitrile for various concentrations. Curve 1 –), 2 – c = 1 mmol L^{-1}, curve 2 – c = 2 mmol L^{-1}, curve 3 – c = 3 mmol L^{-1}, curve 4 – c = 4 mmol L^{-1}, curve 5 – c = 5 mmol L^{-1}.**(B)** Dependence of the anodic peak current on the catechin concentration; curve 1 – v = 0.05 V s^{-1}, curve 2 – v = 0.1 V s^{-1}, curve 3 – v = 0.2 V s^{-1}.

Select voltammograms recorded for different substrate concentrations and the dependence of the anodic peak current on the concentrations are presented in Fig. 4. The potential of peak I of the catechin electro-oxidation shifted towards more positive values with increasing substrate concentration, while the potential f peak II – towards less positive values. Changes in anodic peak currents during the first step of the catechin electrooxidation process were linear in the investigated concentration range. Due to linearity of i_p vs. catechin concentration, the cyclic voltammetry method can be successfully applied to determine catechin concentration. Cyclic voltammograms recorded for different substrate concentration were used to determine the peak potential (E_{pa}), the half-peak potential ($E_{pa/2}$), and the half-wave potential ($E_{1/2}$). The anodic transfer coefficient (bn_b) and the heterogeneous rate constant (k_{bh}) were calculated according to equations presented in the literature [35, 47]. The anodic transfer coefficient for the electrooxidation of catechin is calculated as 0.43±0.05. The heterogeneous rate constant determined from the half-wave potential is $(2.88\pm0.05) \times 10^{-4}$ cm s^{-1}. The structure of catechin has functional OH groups attached to ring structures that can be electrochemically oxidised.

3.4. Oxidation processes of catechin

The distribution of electron charges in a molecule, which determines the reactivity of the positions of a molecule, is not uniform for the compound examined [48, 49]. The molecular orbital energy (E_{HOMO}) was calculated using the AM1 method as determined in the HyperChem software. The calculated energy of the highest filled orbital (E_{HOMO} − ionisation potential) determines the ease of electron release and indicates the sites most susceptible to oxidation (Fig. 5). The structure of catechin has OH groups attached to the rings, which can be electrochemically oxidised. As determined by the distribution of electron charges in the molecule (Fig. 5), the oxidation group OH in ring B is most easily oxidised. The E_{HOMO} for catechin is -8.646 eV.
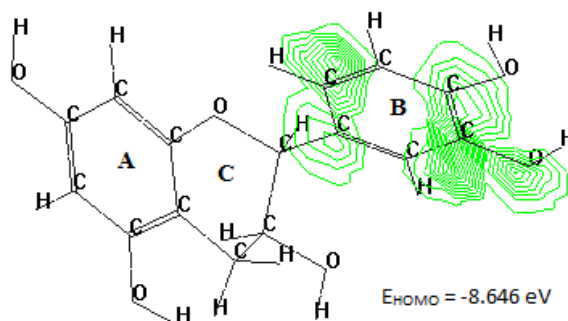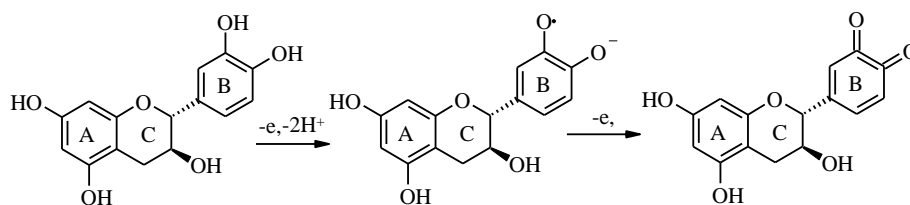

Figure 5. The electron density and probable sites in a catechin molecule susceptible to electrooxidation.

Based on the cyclic voltammetry measurements, quantum chemical calculations, and the literature data [6, 50], the mechanism for the oxidation of catechin was proposed (Scheme 1):

Scheme 1. Proposed mechanism of catechin electrooxidation.

The first step of the electrooxidation process of catechin includes the exchange of one electron and two protons resulting in the formation of a semiquinone. The next step is the exchange of a second electron resulting in the formation a quinone.

3.5. DSC and FTIR spectroscopy of catechin

The melting temperature range was one of the most important parameters for catechin. The melting temperature range of catechin were measured by a differential scanning calorimeter (DSC) with the dynamic measurement method.
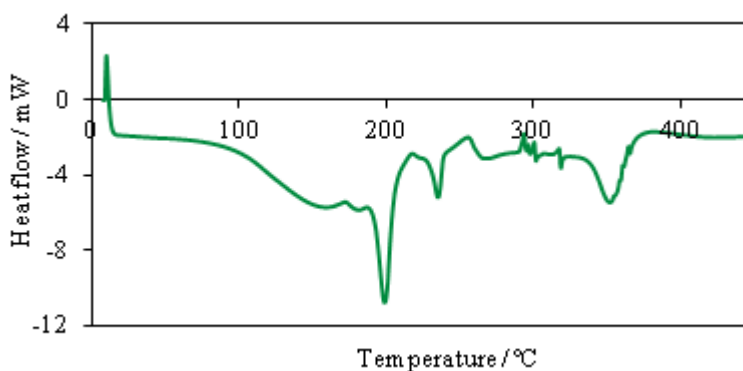

Figure 6. DSC curve of catechin.

The DSC curve of catechin shows two endothermal peaks with onset temperatures of 138 °C (E= 213 J/g) and 175°C (17,9 J/g), which are attributed to the melting of the crystal phase. The third peak of catechin (at 250 °C) is related to a decomposition process with water loss (Figure 6).

FTIR spectroscopy was used to evaluate and analyse this type of compound [51, 52]. Figure 7 shows the spectrum of catechin. The FTIR spectrum shows characteristic peaks of different intensities between 2936 and 458 wavenumber (cm^{-1}) and a broad adsorption OH group peak between 3400 and 3100 cm^{-1}. However, no peak characteristic appeared for the C=O group (quinone), although some changes in the O-H group peaks can be observed (1670–1820 cm^{-1}). The region of 1070–1150 cm^{-1} is characteristic of C-O groups and of the disubstituted aromatic ring, whose peaks normally lie in the range of 1200–900 cm^{-1}.
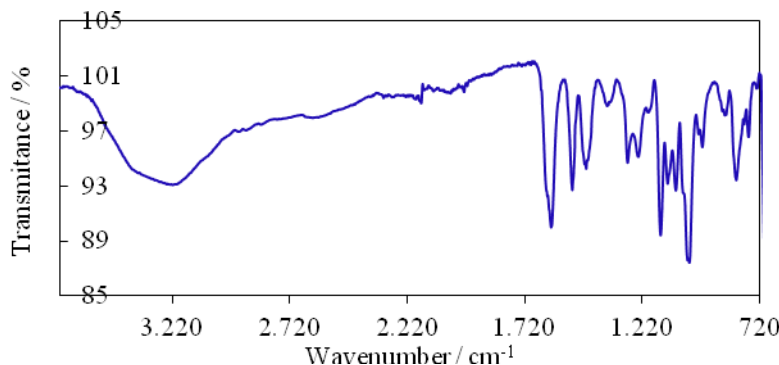
Figure 7. FTIR spectrum of catechin.

4. CONCLUSIONS

The electrochemical behaviour of catechin at a Pt electrode in non-aqueous solution proceeds in at least two electrode steps before the potential reaches a value at which oxygen evolution starts. The peaks on the cyclic voltammograms correspond to the catechin oxidation reaction, which is diffusion controlled. The relationship of the anodic peak current vs. catechin concentration is linear and can be applied to determine the substrate concentration in environmental samples. In non-aqueous media, the anodic transfer coefficient (βn_β) and the rate constant (k_{bh}) were 0.43 and $(2.88\pm0.05) \times 10^{-4}$ cm s^{-1}, respectively.

Based on the experimental results and quantum chemistry calculations, the electrooxidation mechanisms of catechin were proposed. In the first electrochemical step, the hydroxyl group of ring B is oxidised, and one electron and two protons are exchanged resulting in the formation of a semiquinone. The next step is the exchange of a second electron resulting in the formation of a quinone.

The properties of catechin in a homogeneous environment were investigated using DSC and FTIR spectroscopy.

References

1. A. Goodwin, C. E. Banks and R. G. Compton, *Electroanalysis,* 18 (2006) 849.
2. D. Fracassetti, N. Lawrence, A. G. J. Tredoux, A. Tirelli, H. H. Nieuwoudt and W. J. Du Toit, *Food Chem.*, 128 (2011) 1136.
3. A. Rashidinejad, E. J. Birch, D. Sun-Waterhouse and D. W. Everett, *Food Chem.*, 156 (2014) 176.
4. P. A. Kilmartin, H. Zou and A. L. Waterhouse, *J. Agric. Food Chem.*, 49 (2001) 1957.
5. K. Imai, I. Nakanishi, A. Ohno, M. Kurihara, N. Miyata, K. Matsumoto, A. Nakamura and K. Fukuhara, *Bioorg. Med. Chem. Lett.*, 24 (2014) 2582.
6. P. Janeiro and A. M. O. Brett, *Anal. Chim. Acta*, 518 (2004) 109.
7. F. Surco-Laos, M. Dueñas, S. González-Manzano, J. Cabello, C. Santos-Buelga and A. M. González-Paramás, *Food Res. Int.*, 46 (2012) 514.

8. T. M. Rains, S. Agarwal and K. C. Maki, *J. Nutr. Biochem.*, 22 (2011) 1.
9. S. K. Katiyar, *Arch. Biochem. Biophys.*, 508 (2011) 152.
10. Ch. A. Bursill, M. Abbey and P. D. Roach, *Atherosclerosis*, 193 (2007) 86.
11. S. I. Koo, S. K. Noh, *J. Nutr. Biochem.*, 18 (2007) 179.
12. M. Nakayama, N. Shigemune, T. Tsugukuni, H. Jun, T. Matsushita, Y. Mekada, M. Kurahachi and T. Miyamoto, *Food Control*, 25 (2012) 225.
13. A. Sharma, S. Gupta, I. P. Sarethy, S. Dang and R. Gabrani, *Food Chem.*, 135 (2012) 672.
14. W. Zhua and Z. Zhang, *Int. J. Biol. Macromol.*, 70 (2014) 150.
15. D. A. El-Hady, *Anal. Chim. Acta*, 593 (2007) 178.
16. O. Makhotkina and P. A. Kilmartin, *J. Agric. Food Chem.*, 61 (2013) 5573.
17. F. de Souza Dias, M. P. Lovillo, C. G. Barroso and J. M. David, *Microchem. J.*, 96 (2010) 17.
18. M. Šeruga, I. Novak and L. Jakobek, *Food Chem.*, 124 (2011) 1208.
19. H. Arakawa, M. Kanemitsu, N. Tajima and M. Maeda, *Anal. Chim. Acta*, 472 (2002) 75.
20. G. Magarelli, L. H. C. Lima, J. G. da Silva, J. R. SouzaDe and C. S. P. de Castro, *Microchem. J.*, 117 (2014) 149.
21. S. Smarzewska, D. Guziejewski, M Skowron, S. Skrzypek and W. Ciesielski, *Cent. Eur. J. Chem.*, 12 (2014) 1239.
22. N. F. Atta, A. Galal and S. M. Azab, *Int. J. Electrochem. Sci.*, 6 (2011) 5082.
23. E. Wudarska, E. Chrzescijanska, E. Kusmierek and J. Rynkowski, *Electrochim. Acta*, 93 (2013) 189.
24. A. Masek, E. Chrzescijanska and M. Zaborski, *Electrochim. Acta*, 107 (2013) 441.
25. E. Chrzescijanska, E. Wudarska, E. Kusmierek and J. Rynkowski, *J. Electroanal. Chem.*, 713 (2014) 17.
26. G. Ziyatdinova, E. Ziganshina and H. Budnikov, *Electrochim. Acta*, 145 (2014) 209.
27. A. Masek, E. Chrzescijanska, M. Zaborski and M. Maciejewska, *C. R. Chimie*, 15 (2012) 524.
28. R. N. Goyal and S. P. Singh, *Electrochim. Acta*, 51 (2006) 3008.
29. S. K. Moccelini, S. C. Fernandes, T. P. de Camargo, A. Neves and I. C. Vieira, *Talanta*, 78 (2009) 1063.
30. M. S. Maoela, O. A. Arotiba, P. G. L. Baker, W. T. Mabusela, N. Jahed, E. A. Songa and E. I. Iwuoha, *Int. J. Electrochem. Sci.*, 4 (2009) 1497.
31. J. Sochor, J. Dobes1, O. Krystofova, B. Ruttkay-Nedecky, P. Babula, M. Pohanka, T. Jurikova, O. Zitka, V. Adam, B. Klejdus and R. Kizek, *Int. J. Electrochem. Sci.*, 8 (2013) 8464.
32. L. J. Yang, Ch. Tang, H. Y. Xiong, X. H. Zhang and S. F. Wang, *Bioelectrochemistry*, 75 (2009) 158.
33. Y. Yardim, A. Levent, E. Keskin and Z. Şentürk, *Talanta*, 85 (2011) 441.
34. E. Chrzescijanska, E. Kusmierek and G. Nawrat, *Polish J. Chem.*, 83 (2009) 1115.
35. B. Habibi, M. Jahanbakhshi and M. H. Pournaghi-Azar, *Anal. Biochem.*, 411 (2011) 167.
36. C. M. A. Brett and A. M. O. Brett, Electrochemistry: Principles, Methods and Applications, Oxford University Press, New York, 1993, p. 427.
37. A. Masek, E. Chrzescijanska and M. Zaborski, *Int. J. Electrochem. Sci.*, 9 (2014) 7904.
38. A. M. O. Brett and M. E. Ghica, *Electroanalysis*, 159 (2003) 1745.
39. A. Masek, M. Zaborski and E. Chrzescijanska, *Food Chem.*, 127 (2011) 699.
40. B. J. Sanghavi and A. K. Srivastava, *Electrochim. Acta*, 55 (2010) 8638.
41. E. Kusmierek, E. Chrzescijanska, M. Szadkowska-Nicze and J. Kaluzna-Czaplinska, *J. Appl. Electrochem.*, 41 (2011) 51.
42. R. N. Goyal, S. Bishnoi and B. Agrawal, *J. Electroanal. Chem.*, 655 (2011) 97.
43. A. Masek, E. Chrzescijanska and M. Zaborski, *Int. J. Electrochem. Sci.*, 9 (2014) 6809.
44. M. Mazloum-Ardakani and Z. Taleat, *Int. J. Electrochem. Sci.*, 4 (2009) 694.
45. J. C. Abbar, S. J. Malode and S. T. Nandibewoor, *Bioelectrochemistry*, 83 (2012) 1.
46. A. Masek, E. Chrzescijanska and M. Zaborski, *Int. J. Electrochem. Sci.,* 9 (2014) 7875.

47. Z. Galus, Fundamentals of electrochemical analysis, New York: Ellis Horwood; Warsaw: Polish Scientific Publishers PWN, 1994, pp. 84, 297.

48. A. S. Barham, B. M. Kennedy, V. J. Cunnane and M. A. Daous, *Int. J. Electrochem. Sci.*, 9 (2014) 5389.

49. M. M. Kabanda, I. B. Obot and E. E. Ebenso, *Int. J. Electrochem. Sci.*, 8 (2013) 10839.

50. M. Medvidović-Kosanović, M. Šeruga, L. Jakobek and I. Novak, *Croat. Chem. Acta*, 83 (2010) 197.

51. S. B. Jadhav and R. S. Singhal, *Food Chem.*, 150 (2014) 9.

52. S. D. Silva, R. P. Feliciano, L. V. Boas and M. R. Bronze, *Food Chem.*, 150 (2014) 489.